V-Band Monolithic Additive-Manufactured Geodesic Lens Array Antenna

Pilar Castillo-Tapia, *Graduate Student Member, IEEE*, José Rico-Fernández, *Graduate Student Member, IEEE*, and Oscar Quevedo-Teruel, *Fellow, IEEE*

***Abstract*—Fully metallic geodesic lens antennas are popular for millimeter-wave band applications due to their simplicity, robustness, and low loss. Here, we report the experimental results of a geodesic lens array antenna, which was specifically designed to be additive-manufactured in one single piece using laser powder-bed fusion (LPBF). LPBF in aluminum alloy AlSi10Mg is able to produce high conductivity and relatively low surface roughness, so the antenna is highly directive and efficient. In addition, LPBF increases the robustness of the design since the lens array is monolithic, i.e., the risks associated with the assembly, including misalignments and undesired air gaps between pieces, are totally eliminated.**

***Index Terms*—Additive manufacturing (AM), array antenna, geodesic lenses, laser powder-bed fusion (LPBF), lens antenna.**

I. Introduction

GEODESIC lens antennas have shown potential for many applications in the millimeter-wave (mm-wave) regime, such as radars, space, and terrestrial communications. The main advantages of this type of antennas are their multibeam capabilities, high efficiency, and cost-effective manufacturing [1]. A geodesic lens is a homogeneous lens that, by adding a third dimension, mimics the wave path of a planar graded-index lens [2], [3]. To decrease the total height of these lenses, their profile can be mirrored as initially proposed in [4], or modulated as in [5]. Some examples of graded-index lenses that have been implemented into geodesic shapes are the Luneburg [6], half-Luneburg [7], [8]; generalized Luneburg [9]; near-field focusing [10]; half-Maxwell fish-eye [11]; and double-layer reflective lenses [12].

When these lenses are rotationally symmetric, extreme scanning angles, up to $\pm 75^{\circ}$ in one plane, have been reported in the literature [5]. More recently, to scan in two planes, geodesic lens arrays were proposed in [13]. The final design reported in [13] operates in the V-band and has four elements that were manufactured in five identical metallic plates using computer numerical control (CNC) milling. To mitigate the undesired leakage between the plates, glide-symmetric holes were used. Without these holes, the undesired leakage between the feeds would degrade the performance of the antenna as reported for a V-band two-piece geodesic lens antenna in [14].

The aforementioned problems of leakage and misalignment between pieces can be eliminated using additive manufacturing (AM). AM is an emerging manufacturing technique that has proved to be an alternative to conventional subtractive manufacturing methods, such as milling. This manufacturing method was first introduced for weight reduction and improvement of mechanical properties by applying topological optimization. AM has advantages over traditional manufacturing methods in terms of speed, accuracy, and cost effectiveness. In addition, AM permits the creation of conformal and arbitrary shapes that were previously unmanufacturable. Although AM has grown mainly in the mechanical sector, it can also be extrapolated to other areas. One of the new fields where it has aroused special interest is microwave technology.

Antennas and microwave devices can be additively manufactured using three different techniques. The first technique is based on fused deposition melting or stereolithography, which produces plastic parts, which act as dielectric structures. With this technique, graded-index lenses using discretized layers [15], [16], [17] or metasurfaces [18], [19], [20], [21] have been proposed in the literature. The second possibility is to manufacture plastic parts and applying a subsequent metallic coating, commonly nickel [22] or copper [23], [24]. The third option is to manufacture metal-only components using techniques such as binder jetting, laser metal deposition, and laser powder-bed fusion (LPBF).

Here, we will focus in LPBF. This manufacturing technique consists of an application and deposition of layers of metal powder of heights of 20–30 μm using a tool called a recoater. This recoater provides a uniform layer of metal powder on the printing bed, which is then selectively melted by means of an energy source, which in the case of LPBF is a laser. Once the layer of metal powder has been melted, a uniform layer will be added again by the recoater to continue melting the material until the piece is completed. This technique has been recently used for manufacturing microwave components, such as waveguides filters [25], [26] or horn arrays [27]. In addition, it is fully compatible with space applications, and it permits a significant reduction of weight in large structures. In this letter, we demonstrate the potential of this technique

Manuscript received 20 June 2023; accepted 9 July 2023. Date of publication 12 July 2023; date of current version 6 October 2023. The work of Oscar Quevedo-Teruel and Pilar Castillo-Tapia was supported by the VR Project under Grant 2022-03865 through "Research project grant within natural and engineering sciences." *(Corresponding author: Pilar Castillo Tapia.)*

Pilar Castillo-Tapia and Oscar Quevedo-Teruel are with the Division of Electromagnetic Engineering and Fusion Science, KTH Royal Institute of Technology, SE-100 44 Stockholm, Sweden (e-mail: pilarct@kth.se; oscarqt@kth.se).

José Rico-Fernández is with the Northern Waves AB, SE-114 28 Stockholm, Sweden (e-mail: pepe.rico@northern-waves.com).

Digital Object Identifier 10.1109/LAWP.2023.3294541

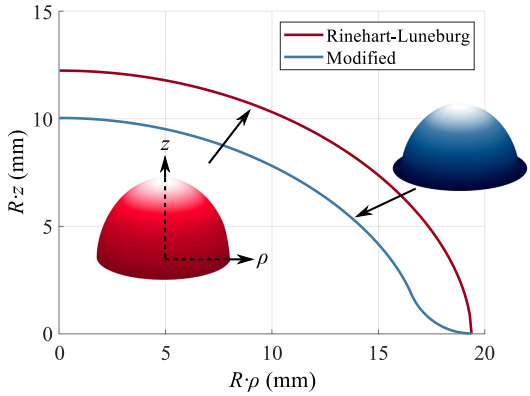

Fig. 1. Lens profile of the Rinehart–Luneburg lens and a modified version with flat transition at the edge.

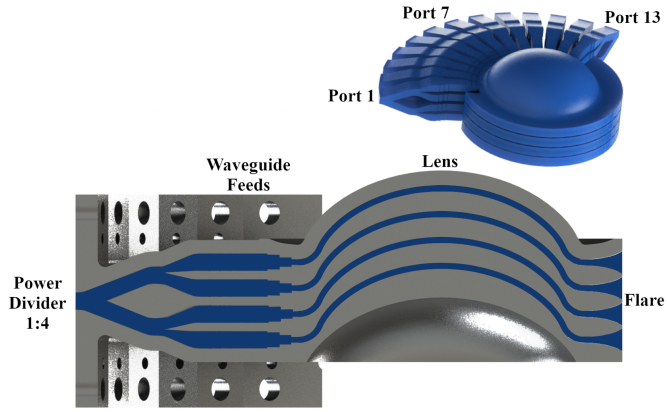

Fig. 2. Cross section and perspective views of the geodesic lens array. Air/vacuum is represented in blue.

with the design, manufacturing, and testing of an array antenna composed of four elements, which are integrated with a 1:4 power divider to provide a uniform phase distribution. This geodesic lens array antenna working in the V-band has been specifically designed to be manufactured in a monolithic piece using AM.

II. Design of the Geodesic Lens Array Antenna

The profile of the Rinehart–Luneburg lens is calculated from the differential equation [28]

$$\mathrm{d}z = \sqrt{\left(\frac{1}{2} + \frac{1}{2\sqrt{1-\rho^2}}\right)^2 - 1}\,\mathrm{d}\rho \tag{1}$$

where ρ is the normalized radial position and z the normalized height. The solution to this equation is represented with red color in Fig. 1 with a radius $R = 19.4$ mm. The almost vertical edge of the Rinehart–Luneburg lens profile cannot be manufactured monolithically using AM, as this technique typically requires overhanging angles not exceeding 45°. In order to fulfill with the manufacturing requirements, the lens profile has been modified so that the four lenses can be stacked and manufactured in a single piece. The new profile is optimized using the ray-tracing model proposed in [29] and it is calculated using the approximation $z = h_0(1-\rho^p)^{1/q}$ with parameters $h_0 = 0.56$ mm, $p = 2$, and $q = 1.6$. A bend of 3.1 mm radius is added at the end of the profile to reduce reflections from the abrupt transition. The modified profile is represented with blue color in Fig. 1.

Thirteen waveguide feeds are added to produce independent beams with a scanning range of 120°. The waveguide feeds have two-stepped transitions that reduce the transversal size of the waveguide, as proposed in [13], although, in this case, they all keep a length of 14.2 mm. At the opposite side of the feeds, an exponential flare is added to match the impedance of the parallel plate waveguide with free space.

The lens antennas are stacked to form an array antenna with four elements with an interelement spacing of 3.5 mm (0.7λ at 60 GHz). The array antenna is integrated with thirteen identical power dividers that distribute the energy between the antenna elements with a uniform phase distribution. This power divider

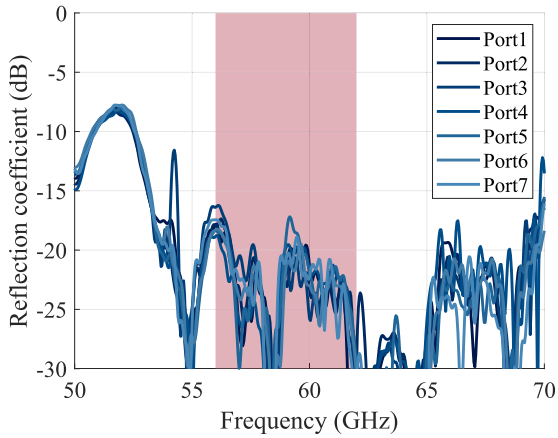

Fig. 3. Simulated reflection coefficient for ports 1–7 of the geodesic lens array illustrated in Fig. 2. Given the symmetry of the antenna, ports 8–13 are omitted.

was previously designed and reported in [13]. It has a 2 dB difference in amplitude between the middle and side elements to reduce the side lobe level (SLL) in the vertical plane of the antenna. A steeper amplitude tapering could be used to further reduced the SLL, but at the cost of a lower aperture efficiency. The model of the final design is shown in Fig. 2. A topological optimization of the metallic part is done to reduce the excess of material and get a more compact and lightweight design. The maximum width of the metallic walls is 2 mm.

The simulated reflection coefficients at ports 1–7 of the designed array antenna are shown in Fig. 3. They are below −15 dB in the frequency band 56–62 GHz.

III. Additive-Manufactured Geodesic Lens Array

Traditionally, the use of subtractive manufacturing (CNC milling) and subsequent assembly of several pieces using screws has been used to produce geodesic lens antennas, including single-lens designs [5], [6], [10], [12], [30] or arrays of lenses [13]. However, this fabrication method has problems when scaling in frequency above the K_a-band, for example in V-band. These problems include misalignment [7] and leakage [14] between pieces. The leakage was mitigated in [13] and [14] with the use of glide-symmetric holes.

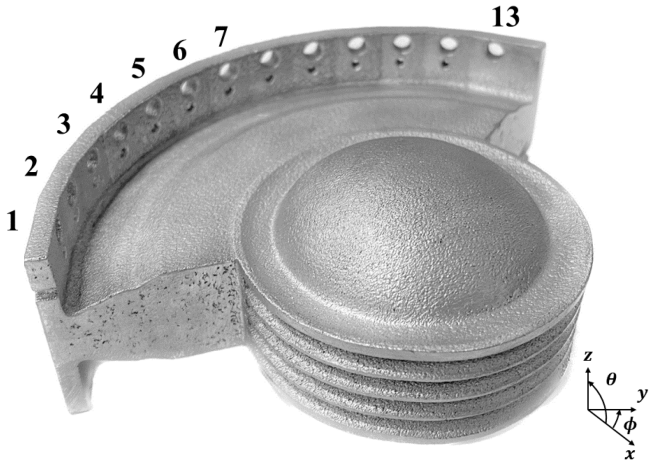

Fig. 4. Geodesic lens array in a V-band prototype manufactured additively in a single piece in aluminum alloy AlSi10Mg.

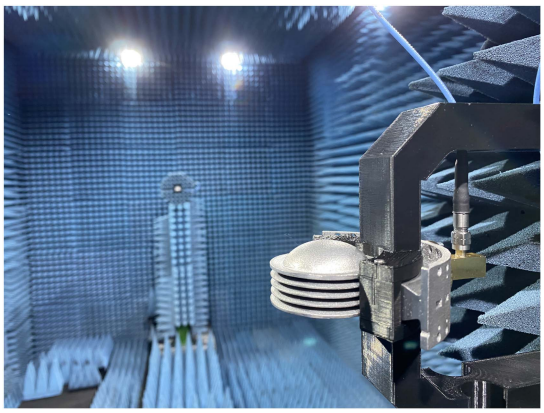

Fig. 5. Measurement setup in the anechoic chamber at KTH, Stockholm, Sweden.

Here, we propose the use of LPBF AM technology, also known as selective laser melting, to obtain a monolithic prototype of the geodesic lens array antenna presented in the previous section. This technique has been recently used to produce a half-Luneburg lens antenna in [8], eliminating the misalignment and leakage between pieces, as previously reported in the literature. However, since it is not possible to reach the inner walls, a postprocessing (like polishing) to reduce the surface roughness cannot be undertaken.

For the design of the V-band geodesic lens array, we decided to use AlSi10Mg aluminium alloy as the material in LPBF due to its electromagnetic and mechanical properties. AlSi10Mg has an electrical conductivity of $\sigma = 1.683501 \times 10^7$ S/m [31] and a surface roughness of $\Delta = 8-10$ μm in the as-built part. The manufactured prototype is illustrated in Fig. 4. To reduce the surface roughness, and ultimately improve the frequency response of the geodesic lens array prototype, the antenna was subjected to two postprocessing treatments. First, we eliminated the manufacturing supports, and we cleaned the antenna in order to avoid errors due to sagging or manufacturing imperfections. Second, the part was subjected to sandblasting with glass microspheres to uniformly reduce the surface roughness to $\Delta = 4-6$ μm.

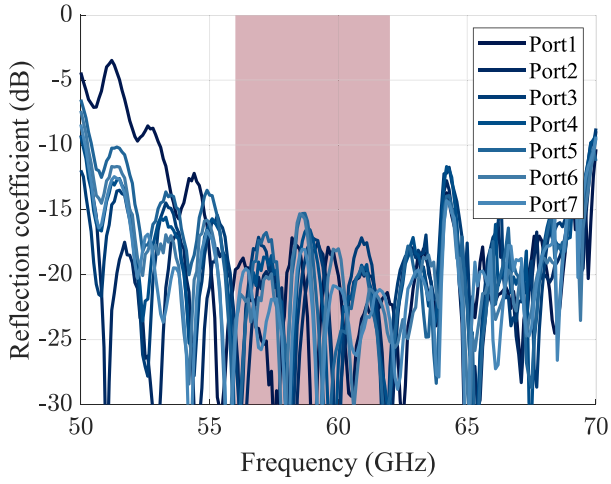

Fig. 6. Measured S-parameters for ports 1–7 of the antenna. Given the symmetry, ports 8–13 have similar results than ports 1–6.

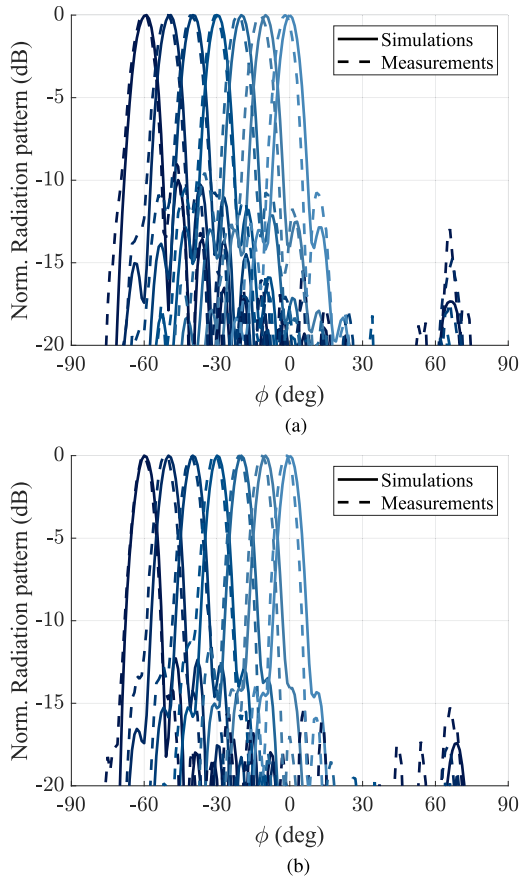

Fig. 7. Simulated and measured radiation patterns at the lowest and highest frequencies of operation, which are 56 and 62 GHz. (a) 56 GHz (lowest frequency). (b) 62 GHz (highest frequency).

IV. Experimental Results

The geodesic lens array prototype was measured in a far-field setup in the anechoic chamber of the Division of

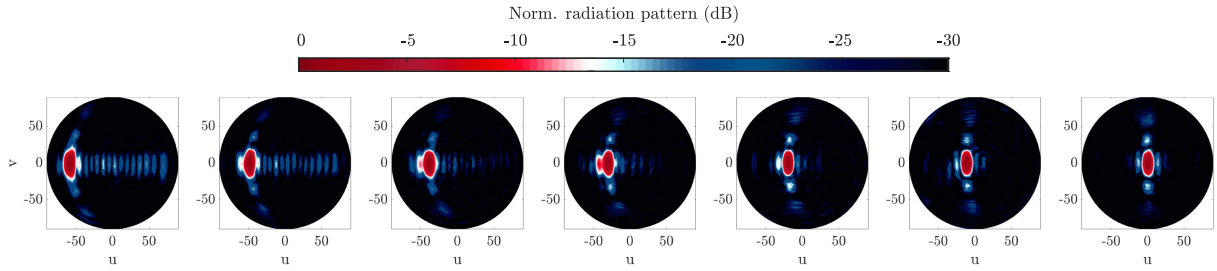

Fig. 8. Normalized radiation patterns at 59 GHz for ports 1 to 7 (left to right).

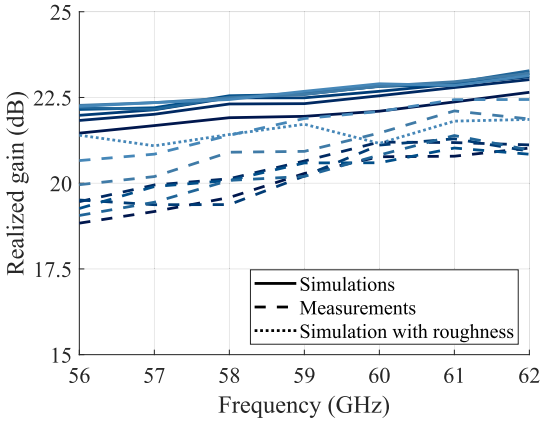

Fig. 9. Simulated (with and without surface roughness) and measured realized gains.

Electromagnetic Engineering and Fusion Science at KTH, as illustrated in Fig. 5. The measured reflection coefficient at ports 1–7 of the antenna is illustrated in Fig. 6. Ports 8–13 have similar results due to the symmetry. In these measurements, time gating was applied to eliminate the reflections between the flange and the antenna. The results demonstrate a low reflection coefficient (below -15 dB) in the full band of operation, 56–62 GHz. The simulated and measured radiation patterns for ports 1–7 are illustrated in Fig. 7. There is a good agreement between simulations and measurements, including a low side lobe level, which is below -10 dB. Similar results were achieved for ports 8–13, although they are omitted here to improve the clarity of the representation.

In Fig. 8, contour plots of the measured radiation patterns are depicted. The SLL are below -10 dB in the horizontal plane and -14 dB in the vertical plane. Finally, the simulated and measured realized gains for ports 1–7 are shown in Fig. 9. The simulated gain (in solid lines) varies between 21.2 and 23.3 dB in the operating frequency band for a lens with conductivity $\sigma = 1.68 \times 10^7$ S/m. The maximum scan losses in simulations are 0.8 dB. The measured gain (in dashed lines) varies between 18.8 and 22.4 dB and the maximum scan losses are 2 dB. This discrepancy to simulations is attributed to the surface roughness of the metallic plates that were not taken into account in simulations. A simulation of port 7 was carried out with 8 μm root mean square (rms) surface roughness as defined in [32]. RMS measures the deviations in the mean surface. As illustrated in Fig. 9 in dotted line, there is a better agreement of this simulation with the measurements.

V. Conclusion

We demonstrated that the use of LPBF AM is suitable for geodesic lens antennas in the V-band. This technique has several advantages associated with the production of monolithic geodesic lens arrays, which avoid undesirable leakage between pieces and misalignment problems. Our experimental results show a reasonably low surface roughness, which resulted in an efficient antenna prototype in the V-band. We can conclude that LPBF can be used to produce low-cost (when compared with milling techniques) geodesic lens antennas in the millimeter-wave band up to 62 GHz.

References

[1] O. Quevedo-Teruel et al., "Geodesic lens antennas for 5G and beyond," *IEEE Commun. Mag.*, vol. 60, no. 1, pp. 40–45, Jan. 2022.
[2] R. F. Rinehart, "A solution of the problem of rapid scanning for radar antennae," *J. Appl. Phys.*, vol. 19, pp. 860–862, Sep. 1948.
[3] R. C. Mitchell-Thomas, O. Quevedo-Teruel, T. M. McManus, S. A. R. Horsley, and Y. Hao, "Lenses on curved surfaces," *Opt. Lett.*, vol. 39, no. 12, pp. 3551–3554, Jun. 2014.
[4] K. S. Kunz, "Propagation of microwaves between a parallel pair of doubly curved conducting surfaces," *J. Appl. Phys.*, vol. 25, no. 5, pp. 642–653, 1954.
[5] N. J. G. Fonseca, Q. Liao, and O. Quevedo-Teruel, "Equivalent planar lens ray-tracing model to design modulated geodesic lenses using non-Euclidean transformation optics," *IEEE Trans. Antennas Propag.*, vol. 68, no. 5, pp. 3410–3422, May 2020.
[6] Q. Liao, N. J. G. Fonseca, and O. Quevedo-Teruel, "Compact multibeam fully-metallic geodesic Luneburg lens antenna based on non-Euclidean transformation optics," *IEEE Trans. Antennas Propag.*, vol. 66, no. 12, pp. 7383–7388, Dec. 2018.
[7] N. J. G. Fonseca, Q. Liao, and O. Quevedo-Teruel, "Compact parallel-plate waveguide half-Luneburg geodesic lens in the Ka-band," *Microw., Antennas Propag.*, vol. 15, no. 2, pp. 123–130, 2021.
[8] J. Rico-Fernández, F. V. Vidarsson, M. Arrebola, N. J. G. Fonseca, and O. Quevedo-Teruel, "Compact and lightweight additive manufactured parallel-plate waveguide half-Luneburg geodesic lens multiple-beam antenna in the Ka-band," *IEEE Antennas Wireless Propag. Lett.*, vol. 22, no. 4, pp. 684–688, Apr. 2023.
[9] O. Zetterstrom et al., "V-band geodesic generalized Luneburg lens antenna with high beam crossover gain," *IEEE Trans. Antennas Propag.*, early access, Jun. 09, 2023, doi: 10.1109/TAP.2023.3283138.
[10] O. Orgeira, G. León, N. J. G. Fonseca, P. Mongelos, and O. Quevedo-Teruel, "Near-field focusing multibeam geodesic lens antenna for stable aggregate gain in far-field," *IEEE Trans. Antennas Propag.*, vol. 70, no. 5, pp. 3320–3328, May 2022.
[11] S. Yang, Q. Chen, F. Mesa, N. J. G. Fonseca, and O. Quevedo-Teruel, "Geodesic half-Maxwell fish-eye lens antenna," *IEEE Trans. Antennas Propag.*, vol. 71, no. 3, pp. 2330–2338, Mar. 2023.
[12] Q. Chen, S. Horsley, N. Fonseca, T. Tyc, and O. Quevedo-Teruel, "Double-layer geodesic and gradient-index lenses," *Nature Commun.*, vol. 13, 2022, Art. no. 2354.
[13] P. Castillo-Tapia et al., "Two-dimensional beam steering using a stacked modulated geodesic Luneburg lens array antenna for 5G and beyond," *IEEE Trans. Antennas Propag.*, vol. 71, no. 1, pp. 487–496, Jan. 2023.

[14] O. Zetterstrom, M. Petek, P. Castillo-Tapia, A. Palomares-Caballero, N. J. G. Fonseca, and O. Quevedo-Teruel, "V-band fully metallic geodesic Luneburg lens antenna," *IEEE Trans. Antennas Propag.*, vol. 71, no. 2, pp. 1965–1970, Feb. 2023.

[15] Z. Larimore, S. Jensen, A. Good, A. Lu, J. Suarez, and M. Mirotznik, "Additive manufacturing of Luneburg lens antennas using space-filling curves and fused filament fabrication," *IEEE Trans. Antennas Propag.*, vol. 66, no. 6, pp. 2818–2827, Jun. 2018.

[16] J. Poyanco, F. Pizarro, and E. Rajo-Iglesias, "Cost-effective wideband dielectric planar lens antenna for millimeter wave applications," *Sci. Rep.*, vol. 12, no. 1, 2022, Art. no. 4204.

[17] J. Melendro-Jimenez, P. Sanchez-Olivares, A. Tamayo-Dominguez, X. Sun, and J. M. Fernandez-Gonzalez, "3D printed directive beam-steering antenna based on gradient index flat lens with an integrated polarizer for dual circular polarization at W-band," *IEEE Trans. Antennas Propag.*, vol. 71, no. 1, pp. 1059–1064, Jan. 2023.

[18] V. M. Pepino, A. F. da Mota, A. Martins, and B.-H. V. Borges, "3D-printed dielectric metasurfaces for antenna gain improvement in the Ka-band," *IEEE Antennas Wireless Propag. Lett.*, vol. 17, no. 11, pp. 2133–2136, Nov. 2018.

[19] J.-M. Poyanco, O. Zetterstrom, P. Castillo-Tapia, N. J. G. Fonseca, F. Pizarro, and O. Quevedo-Teruel, "Two-dimensional glide-symmetric dielectric structures for planar graded-index lens antennas," *IEEE Antennas Wireless Propag. Lett.*, vol. 20, no. 11, pp. 2171–2175, Nov. 2021.

[20] O. Zetterstrom, N. J. G. Fonseca, and O. Quevedo-Teruel, "Compact half-Luneburg lens antenna based on a glide-symmetric dielectric structure," *IEEE Antennas Wireless Propag. Lett.*, vol. 21, no. 11, pp. 2283–2287, Nov. 2022.

[21] Y. Kim, R. Phon, E. Park, and S. Lim, "An additively manufactured deployable broadband metasurface lens antenna," *IEEE Antennas Wireless Propag. Lett.*, vol. 22, no. 7, pp. 1672–1676, Jul. 2023.

[22] A. Rebollo, A. F. Vaquero, M. Arrebola, and M. R. Pino, "3D-printed dual-reflector antenna with self-supported dielectric subreflector," *IEEE Access*, vol. 8, pp. 209091–209100, 2020.

[23] A. Dorlé et al., "Additive manufacturing of modulated triple-ridge leaky-wave antenna," *IEEE Antennas Wireless Propag. Lett.*, vol. 17, no. 11, pp. 2123–2127, Nov. 2018.

[24] T. Skaik et al., "Evaluation of 3D printed monolithic G-band waveguide components," *IEEE Trans. Compon., Packag., Manuf. Technol.*, vol. 13, no. 2, pp. 240–248, Feb. 2023.

[25] M. González-Calvo, J. R. Montejo-Garai, J. A. Ruiz-Cruz, and J. M. Rebollar, "Additive manufacturing of a high-performance Q-band circular TE01 mode flared-type transducer," *IEEE Microw. Wireless Compon. Lett.*, vol. 29, no. 9, pp. 577–579, Sep. 2019.

[26] R. Salazar, F. Pizarro, D. Vasquez, and E. Rajo-Iglesias, "Assessment of 3D-printed waveguides using conductive filaments and a chloroform-based smoothing process," *Additive Manuf.*, vol. 51, 2022, Art. no. 102593.

[27] L. Alonso-González, J. Rico-Fernández, A. F. Vaquero, and M. Arrebola, "Millimeter-wave lightweight 3D-printed 4×1 aluminum array antenna," in *Proc. 16th Eur. Conf. Antennas Propag.*, 2022, pp. 1–5.

[28] M. Šarbort and T. Tyc, "Spherical media and geodesic lenses in geometrical optics," *J. Opt.*, vol. 14, no. 7, 2012, Art. no. 075705.

[29] Q. Liao, N. J. G. Fonseca, M. Camacho, A. Palomares-Caballero, F. Mesa, and O. Quevedo-Teruel, "Ray-tracing model for generalized geodesic multiple beam lens antennas," *IEEE Trans. Antennas Propag.*, vol. 71, no. 3, pp. 2640–2651, Mar. 2023.

[30] F. V. Vidarsson et al., "Conformal parallel plate waveguide polarizer integrated in a geodesic lens antenna," *IEEE Trans. Antennas Propag.*, vol. 70, no. 11, pp. 10327–10337, Nov. 2022.

[31] C. Silbernagel, I. Ashcroft, P. Dickens, and M. Galea, "Electrical resistivity of additively manufactured AlSi10Mg for use in electric motors," *Additive Manuf.*, vol. 21, pp. 395–403, 2018.

[32] D. M. Pozar, *Microwave Engineering*. Hoboken, NJ, USA: Wiley, 2012.